# An automatic land covers identification based on Dempster-Shafer theory for multi-spectral images

Na Li, Arnaud Martin, Rémi Estival

# An automatic land covers identification based on Dempster-Shafer theory for multi-spectral images

Na Li
Univ Rennes, CNRS, IRISA
Total
France
Email: li.na@irisa.fr

Arnaud Martin
Univ Rennes, CNRS, IRISA
France
Email: arnaud.martin@irisa.fr

Rémi Estival
Total, Innovative acquisition
France
Email: remi.estival@total.com

***Abstract*—Several methods have been proposed for land covers classification of remote sensing images. However, for some complex and hard-to-access areas, collecting ground truth for supervised learning approaches is a hazard, expensive and time-consuming. Therefore, we focus on the automatic identification of land covers through specific features extracted from spectral bands. In this paper, we proposed a land covers identification method based on Dempster-Shafer theory, which is fully automatic to infer the semantic sense of labels without any manually labeling processing. Our contributions include an efficient method to extract vegetation through NDVI (Normalized Different Vegetation Index) and an automatic land cover identification using Dempster-Shafer theory.**

***Index Terms*—Spectral index, multi-spectral image, Dempster-Shafer theory.**

## I. Introduction

Spectral index is one of the most essential techniques in land cover identification and change detection using satellite images. However, no universal thresholds of spectral index exist to identify land covers and plenty of ground truth is required to verify various thresholds manually as well. Since different land covers may possess similar spectra, obtaining accurate classification results through traditional machine learning methods becomes difficult. Significant progress has been made recently in developing more powerful classifiers based on spectral properties to extract land covers [1], [2].

Complementary information of identified objects in land cover classification potentially allows a higher classification accuracy. The theory of belief functions, also called Dempster-Shafer theory, has been wildly used in data fusion as a method at the decision level. It performs well in merging classification results from multiple sources, owing to the measurement of uncertainty and imprecision [3]. Dempster-Shafer theory has also been used to relax Bayesian decisions given by a Markovian classification algorithm (ICM), which shows satisfying performances in the classification of very noisy remote sensing images [4]. In general, Dempster-Shafer theory is usually utilized to fuse classification results from supervised learning, while it is also promising to apply it in a fully unsupervised context. In [5], the authors proposed a fusion of two unsupervised learning methods performing well in separating land covers.

In this paper, we propose a new automatic land covers identification method based on the fusion of different one-versus-all classifiers. This paper is organized as follows: in section II, some bases of Dempster-Shafer theory are recalled, followed by the explanation of four classification methods explained in section III. Section IV presents the principal methodology, including construction of mass function. Then, section V illustrates results of experiments. Conclusions are drawn in section VI.

## II. Dempster-Shafer theory

As a generalization of traditional probability, Dempster-Shafer theory [6], [7] allows distributing support for the proposition not only to a single proposition itself but also to the union of propositions that include it. The mass function is defined on all the subsets of the frame of discernment $\Omega = \{\omega_1, \ldots, \omega_n\}$, and assigns belief degree to all the elements in the power set of discernment, noted as $2^\Omega$.

The mass function of the null proposition $\emptyset$ is usually set to zero but it is also possible to be a positive value. The sum of the masses of all the propositions is one:

$$\sum_{A \subseteq \Omega} m(A) = 1 \tag{1}$$

and $m(\emptyset) = 0$.

In order to combine independent sources, the main combination rule is the conjunctive rule given $\forall A \subseteq \Omega$, by:

$$m_{\text{conj}}(A) = \sum_{X_1 \cap \cdots \cap X_S = A} \prod_{s=1}^{S} m_s(X_s), \tag{2}$$

where $s$ represents the different sources from 1 to $S$.

For the decision step, the pignistic probability [8] is currently used because it offers a good compromise between the maximum of credibility and the maximum of plausibility. The basic idea of pignistic probability $\text{betP}$ is to dissipate the mass values associated with focal elements to a specified focal element, which has been generalized in Dempster-Shafer framework, given by:

$$\text{betP}(A) = \sum_{B \in 2^\Omega, B \cap A \neq \emptyset} \frac{1}{|B|} \frac{m(B)}{1 - m(\emptyset)} \tag{3}$$

where $|B|$ represents the cardinality of $B$.

## III. Land covers identification

In this section, we present four one-versus-all detection methods, which can automatically extract one or more specific land covers based on information from different spectral index.

### A. Water detection

As water has the strongest absorption in NIR channel, its NIR reflection can show a great difference compared to other land covers. Based on this property, a threshold can be extracted to identify water and non-water [9]. The method is briefly explained as follows:

1) Find the two first local peaks in the NIR histogram.
2) Use a five-degree polynomial function to approximate the part between the two local peaks.
3) Find the minimal of the five-degree polynomial approximation and use its correspondent NIR value as the threshold of water.

### B. Bare soil detection

Bare soil shows linear relationship between the NIR and Red, called the soil line [10]:

$$NIR = \beta_1 R + \beta_0 \tag{4}$$

This specific property can be applied to extract bare soil as follows:

1) Extract the soil line automatically through the method in [11].
2) Pixels near to the soil line in certain distance $d$ are label as bare soil.

### C. Vegetation detection

This vegetation detection method is based on NDVI, which ranges from $-1$ to 1, to indicate distinct land covers. Vegetation, for example, usually reflects positive values in NDVI while negative values correspond to water. The thresholds of vegetation in NDVI should be carefully selected out through labeled samples in traditional approaches, which is time-consuming. Therefore, we proposed an automatic method without labeled samples to detect vegetation threshold in NDVI. The details of the method are as follows:

1) Find a threshold $thr_0$ in NDVI and another threshold $thr_i$ with $i = 1$ in the NDVI interval $[thr_0,1]$ through Otsu method [12].
2) Find a threshold $thr_{i+1}$ in the NDVI interval $[thr_i,1]$ through Otsu method until $thr_{i+1}$ is equal or very close to $thr_i$, and keep all the thresholds detected in the threshold list.
3) In the interval $[thr_0,thr_1]$, Otsu method is applied to find a new threshold $thr_n$. If $thr_n < thr_1$, $thr_n$ is inserted after $thr_0$ in the list as the new $thr_1$. Continue to insert threshold until $thr_1$ is equal or very close to $thr_0$.
4) Calculate the first order of difference of the threshold list, noted as $dif$.
5) Use a three-degree polynomial function to approximate $dif$ and the NDVI value corresponds to the maximal of the polynomial function is the final threshold $thr$ to extract vegetation.

All pixels with superior NDVI value than $thr$ are labeled as vegetation while the rest pixels are non vegetation.

### D. Water and Impervious surface detection

Biological Complex Index (BCI) is a spectral index ranging from $-1$ to 1 [13]. It indicates vegetation with negative values, bare soil with values around zero and impervious surface with positive values. However, due to the similarity of water and impervious surface in BCI, the detection of only impervious surface requires masking water out firstly.

Considering all classifiers in the one-against-all structure should be independent, we keep the water with impervious surface in this classifier as the same class. The proposed water and impervious detection are illustrated as follows:

1) For all pixels with positive BCI values, Otsu method is applied to find a threshold, noted as $thr_t$.
2) Apply Otsu method again in the BCI interval $(0,thr_t]$ to find the final threshold $thr$.
3) Pixels with BCI values superior to $thr$ are labeled as 'water and impervious surface', and BCI values inferior to $thr$ labeled as 'the rest land covers'.

## IV. Fusion of detection methods

The discernment frame is defined as $\Omega = \{\omega_1, \omega_2, \omega_3, \omega_4\}$ where $\omega_1$ represents 'water', $\omega_2$ 'bare soil', $\omega_3$ 'vegetation', $\omega_4$ 'impervious'. For these four methods presented in section III, we denote water detection as $A$, bare soil detection as $B$, vegetation detection as $C$, water and impervious surface detection as $D$. Two classes generated by the four methods in the discernment frame are shown in table I:

TABLE I: Classes from each classifier in discernment frame

| Method | feature space | class 1 | class 2 |
|---|---|---|---|
| $A$ | NIR | $\omega_1$ | $\omega_2 \cup \omega_3 \cup \omega_4$ |
| $B$ | NIR,Red | $\omega_2$ | $\omega_1 \cup \omega_2 \cup \omega_4$ |
| $C$ | NDVI | $\omega_3$ | $\omega_1 \cup \omega_2 \cup \omega_4$ |
| $D$ | BCI | $\omega_1 \cup \omega_4$ | $\omega_2 \cup \omega_3$ |

For the methods $A$, $C$, $D$, a threshold in their corresponding feature space is found to separate the discernment frame into two classes. Therefore, the principle to assign mass functions are the same for these three methods: a pixel is closer to the threshold, its label is more uncertain.

For method $A$, $T_{NIR}$ is the threshold in NIR. The mass functions for pixel $x$ with value $nir$ of NIR are as follows:

$$\begin{cases} m_A(\{\omega_1\}) = \frac{\alpha}{N}\left(1 - e^{-\frac{T_{NIR}-nir}{t_{NIR}-nir_{min}}}\right) \\ m_A(\{\omega_2 \cup \omega_3 \cup \omega_4\}) = \frac{\alpha}{N}\left(1 - e^{-\frac{nir-T_{NIR}}{nir_{max}-T_{NIR}}}\right) \\ m_A(\Omega)(x) = 1 - m_A(\{\omega_1\}) - m_A(\{\omega_2 \cup \omega_3 \cup \omega_4\}) \end{cases} \tag{5}$$

$N$ is a normalization coefficient to make mass value range from 0 to 1, given by $N = 1 - e^{-1}$. $nir_{min}$ and $nir_{max}$ is the minimal and maximum value of $nir$.

Similarity, we calculate mass functions of mathod C and method D as follows:

$$\begin{cases} m_C(\{\omega_3\}) = \frac{\alpha}{N}\left(1 - e^{-\frac{(ndvi - T_{NDVI})}{T_{NDVI} - ndvi_{min}}}\right) \\ m_C(\{\omega_1 \cup \omega_2 \cup \omega_4\}) = \frac{\alpha}{N}\left(1 - e^{-\frac{ndvi - T_{NDVI}}{ndvi_{max} - T_{NDVI}}}\right) \\ m_C(\Omega) = 1 - m_C(\{\omega_3\}) - m_C(\{\omega_1 \cup \omega_2 \cup \omega_4\}) \end{cases} \quad (6)$$

$$\begin{cases} m_D(\{\omega_1 \cup \omega_4\}) = \frac{\alpha}{N}\left(1 - e^{-\frac{(bci - T_{BCI})}{T_{BCI} - BCI_{min}}}\right) \\ m_D(\{\omega_2 \cup \omega_3\}) = \frac{\alpha}{N}\left(1 - e^{-\frac{(T_{BCI} - bci)}{bci_{max} - T_{BCI}}}\right) \\ m_D(\Omega) = 1 - m_D(\{\omega_1 \cup \omega_4\}) - m_D(\{\omega_2 \cup \omega_3\}) \end{cases} \quad (7)$$

For all pixels labeled as bare soil by method $B$, if they are more closer to the soil line, their labels are more certain. For all pixels labeled as non bare soil, if they are more far away from the soil line,their labels are more certain.

$$\begin{cases} m_B(\{\omega_2\}) = \frac{\alpha}{N}\left(1 - e^{-\frac{d(x,L)_{max} - d(x,L)}{d(x,L)_{max}}}\right) \\ m_B(\{\omega_1 \cup \omega_3 \cup \omega_4\}) = \frac{\alpha}{N}\left(1 - e^{-\frac{d(x,L)}{d(x,L)_{max}}}\right) \\ m_B(\Omega) = 1 - m_B(\{\omega_2\}) - m_C(\{\omega_1 \cup \omega_3 \cup \omega_4\}) \end{cases} \quad (8)$$

where $d(x, L)$ is the euclidean distance between $x$ and the soil line $L$ in NIR-Red plane.

After modeling mass functions, conjunctive rule is utilized to combine the results and maximum of pignistic probability is applied as the decision rule to obtain the basic land covers: vegetation, bare soil, water, and impervious surface. For vegetation and impervious surface, their colors become darker when BCI is approaching to 0. We can directly apply K-means with $k = 3$ on vegetation and impervious surface detected previously to separate the original class into dark, middle and bright sub-groups. The work-flow of the proposed identification method is shown in figure 1.

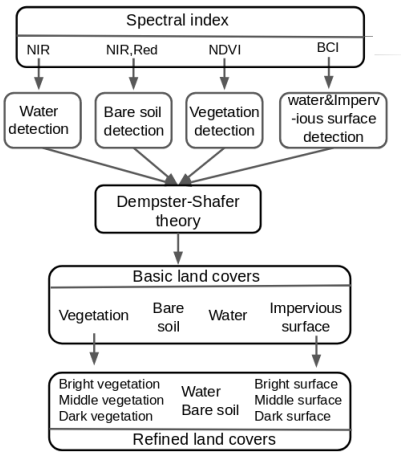


Fig. 1: Work-flow of the proposed method

## V. Experiments and results

Our experiments were conducted in 4 bands (blue, green, red, NIR) of WorldView-2 data from a study area located in Papua New Guinea. The original false color composite image is shown in figure 2. Vegetation appears red, while water corresponds to dark brown or black. Bare soils, roads and building appear in light brown compared to water.

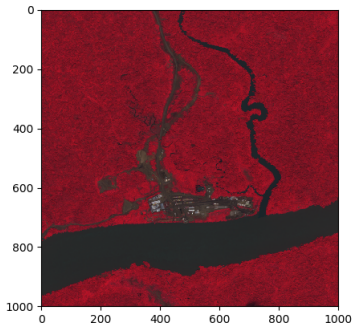


Fig. 2: False color composite of WorldView2 image.

We first applied Dempster-Shafer theory to combine results of the four detection methods presented previously, which renders identification of four basic land cover: water, vegetation, bare soil, and impervious surface. Based on this identification, we refined vegetation and impervious surface in terms of their brightness, thus generating more semantic labels.

Due to the lack of ground truth, we evaluated our method from the aspect of clustering, and compared the results with two clustering methods: K-means and Gaussian Mixture Model (GMM) as shown in figure 3 and table II. Silhouette score which focuses on the measurement of compactness, various and density of clusters was thus applied to evaluate the methods. This score is bounded between $-1$ for incorrect clustering and $+1$ for highly dense and well separated clustering.

TABLE II: Silhouette score of different methods

| | K-means | GMM | The proposed method |
|---|---|---|---|
| Basic land covers | 0.544 | 0.494 | 0.551 |
| Refined land covers | 0.458 | 0.406 | 0.476 |

For the basic land covers, K-means and GMM were utilized with the number of cluster $k = 4$. Identifying vegetation as an entire cluster is evidently difficult for K-means and GMM because spectral dissimilarity is not sufficient to make vegetation distinguishable compared to bare soil, water and impervious surface. The proposed method, on the contrary, automatically generates semantic labels and also has higher silhouette score than the others, which indicating the four land covers rendered by our method is also better defined as clusters.

Vegetation and impervious surface are refined to more detailed classes according to the brightness. Compared with K-means and GMM with $k = 8$, our method still has

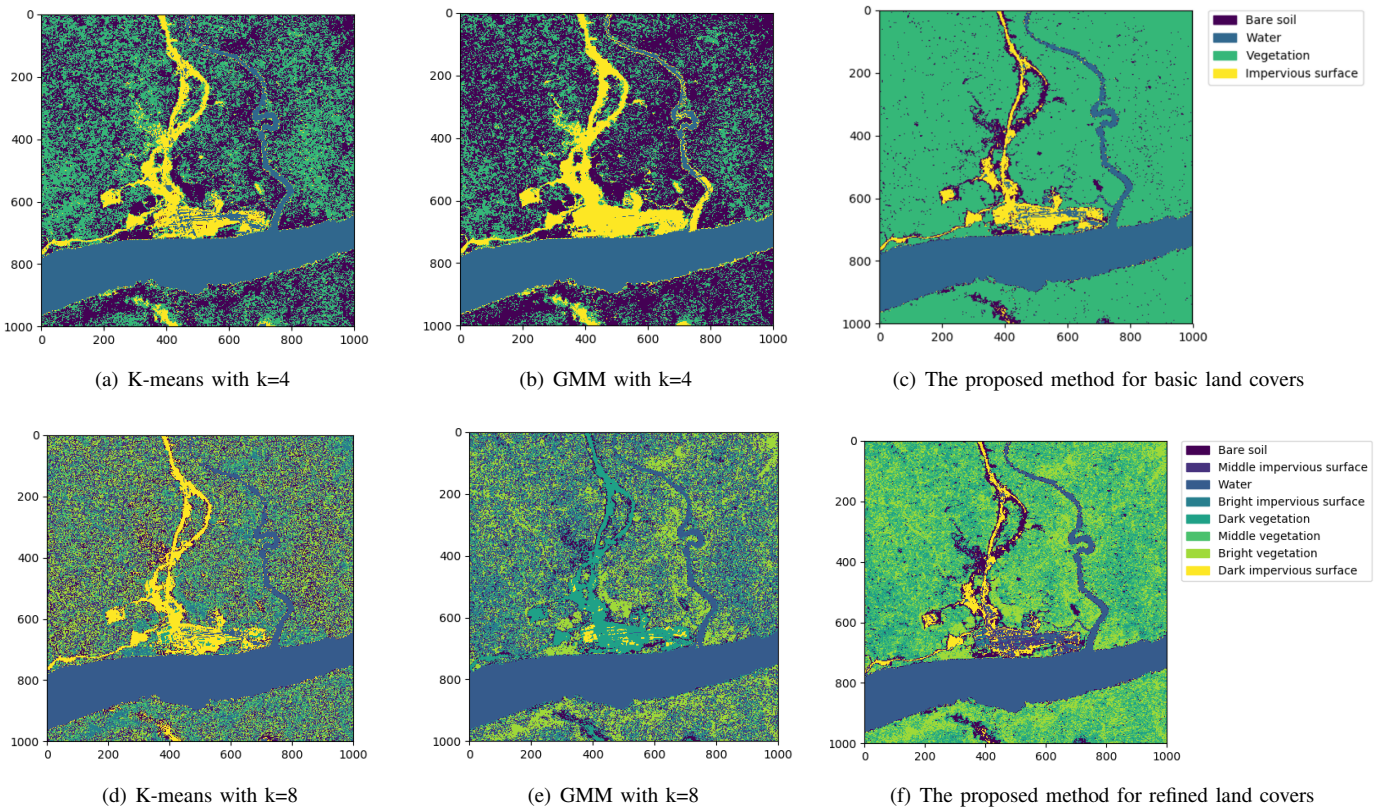


(a) K-means with k=4 (b) GMM with k=4 (c) The proposed method for basic land covers

(d) K-means with k=8 (e) GMM with k=8 (f) The proposed method for refined land covers

Fig. 3: Results of K-means, GMM and the proposed method

better performance in regrouping original data and generates semantic labels for every clusters.

We also verify the proposed method through the comparison of the original multi-spectral images and identification results manually through ENVI, a specific software for processing and analyzing geospatial imagery. The proposed method satisfyingly distinguishes the basic and also refined land covers. Water including a river and even some small streams is well identified. Vegetation and impervious surface with various brightness also greatly identified, which can be observed directly in ENVI. Bare soil near the road is also satisfyingly detected, while it is hard to observe when merging with vegetation.

## VI. Conclusion

In this paper, we proposed an automatic land covers identification method with satisfying performances, which can be applied on the situation where ground truth is unavailable while semantic labels are required. Our future work will focus on the combination of supervised learning and unsupervised learning by Dempster-Shafer theory in remote sensing classification.

## References

[1] S. Neil, B. Timothy, and P. Christopher. Classifying the neotropical savannas of belize using remote sensing and ground survey. *Journal of Biogeography*, 33(3):476–490, 2006.

[2] Sohn Y and Rebello NS. Supervised and unsupervised spectral angle classifiers. *Photogramm Eng Remote Sens*, 68(1):28 – 44, 2013.

[3] A. Martin and E. Radoi. Effective atr algorithms using information fusion models. In *Fusion 2004: Seventh International Conference on Information Fusion*, 2004.

[4] S. Foucher, M. Germain, J. M. Boucher, and G.B. Benie. Multisource classification using icm and dempster-shafer theory. *IEEE Transactions on Instrumentation and Measurement*, 51(2):277–281, Apr 2002.

[5] Le Hegarat-Mascle S., I. Bloch, and D. Vidal-Madjar. Application of dempster-shafer evidence theory to unsupervised classification in multisource remote sensing. *IEEE Transactions on Geoscience and Remote Sensing*, 35(4):1018–1031, Jul 1997.

[6] A. P. Dempster. Upper and lower probabilities induced by a multivalued mapping. *Ann. Math. Statist.*, 38(2):325–339, 04 1967.

[7] G. Shafer. *A Mathematical Theory of Evidence*. Princeton University Press, Princeton, 1976.

[8] Ph. Smets. Constructing the pignistic probability function in a context of uncertainty. In *Proceedings of the Fifth Annual Conference on Uncertainty in Artificial Intelligence*, UAI '89, pages 29–40, Amsterdam, The Netherlands, The Netherlands, 1990. North-Holland Publishing Co.

[9] G. Tetteh and M. Schnert. Automatic generation of water masks from rapideye images. *Journal of Geoscience and Environment Protection*, 3(5):17–23, 2015.

[10] F. Baret, S. Jacquemoud, and J. F. Hanocq. The soil line concept in remote sensing. *Remote Sensing Reviews*, 7(1):65–82, 1993.

[11] Garey A. Fox, G. J. Sabbagh, S. W. Searcy, and C. Yang. An automated soil line identification routine for remotely sensed images. *Soil Science Society of America Journal*, 68(4):1326–1331, 2004.

[12] N. Otsu. A Threshold Selection Method from Gray-level Histograms. *IEEE Transactions on Systems, Man and Cybernetics*, 9(1):62–66, 1979.

[13] D. Chengbin and W. Changshan. Bci: A biophysical composition index for remote sensing of urban environments. *Remote Sensing of Environment*, 127:247 – 259, 2012.